

Supplementary material

485 Forward model grid

We use a coordinate system with nodes along the ice flux lines, based on the work of Parrenin and Hindmarsh (2007). It has the advantage that particle trajectories follow the nodes of the grid and therefore are trivial to calculate, reducing computation time. However, this means that the forward model requires an irregular grid which changes with each new set of parameters tested during the optimisation. The inverse model (where inferred parameters \bar{a} , p and H_m are defined) and observation (radar isochrones for comparison) grids are regular in the (x, Depth) coordinate system, though with a different number of nodes. 490 The interpolation between the forward and inverse model grids thus introduces uncertainties, especially further from the dome, where the forward model grid is coarse. We reduced uncertainty by increasing the resolution of the forward model, so the grid is fine even near the end of the flow line, where the BELDC drill site is located.

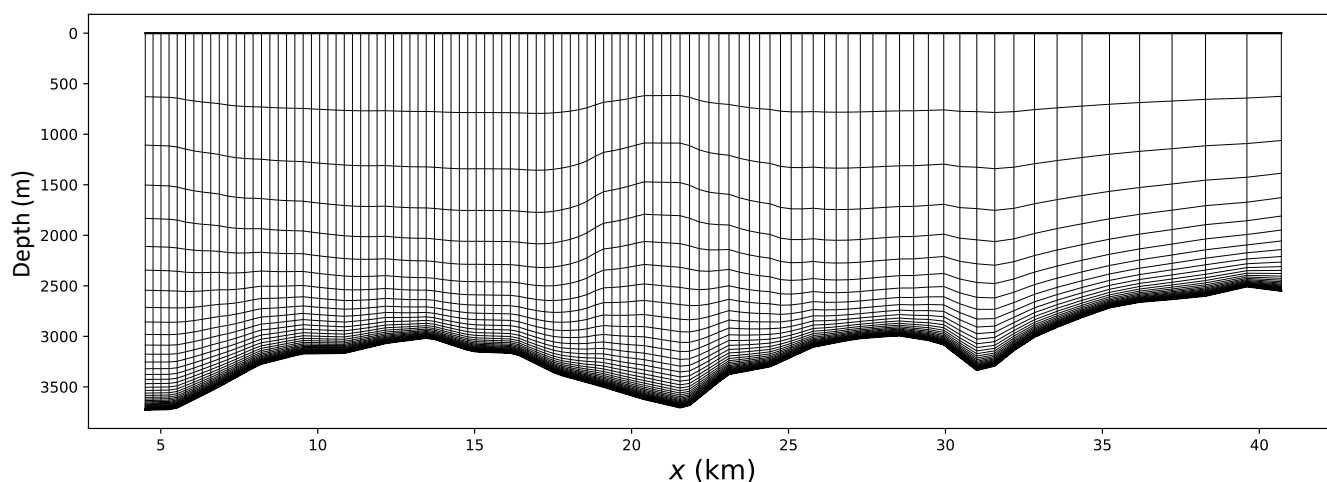


Figure S1. Grid used in the forward model which is regular in the forward model coordinate system, but is shown here in the physical coordinate system (x, Depth) . This figure is for illustrative purposes only, the grid used in the final forward model has 600 nodes in the x direction, more than are shown here.

GNSS surface velocities

Station	Latitude (°S)	Longitude (°E)	Horizontal velocity v (mm yr ⁻¹)	σ_v (mm yr ⁻¹)	Azimuth (°)
GPS1	75.34232	122.27677	71.7	±0.8	241
GPS2	75.30740	122.16995	97.5	±1.6	264
GPS3	75.27960	122.31078	83.5	±0.3	266
GPS4	75.31447	122.41796	63.0	±1.0	228
LCAT	75.28898	122.54462	49.6	±0.7	223
LDC3	75.33861	122.51726	72.0	±0.8	200
LDC4	75.37072	122.47751	88.7	±0.6	196
LDC5	75.39368	122.36740	101.8	±2.1	196
LDC6	75.35578	122.21080	83.0	±0.8	233
LDC7	75.31261	122.11644	98.3	±0.8	264
LDC8	75.28692	122.43745	53.9	±0.6	247
LDC9	75.27775	122.19370	108.4	±0.7	270
LDCC	75.31098	122.29347	78.0	±0.3	251
NECK	75.26738	122.73825	37.6	±0.6	206

Table S1. GNSS control points positions and velocities (International Terrestrial Reference Frame 2014). Azimuth is relative to true north.

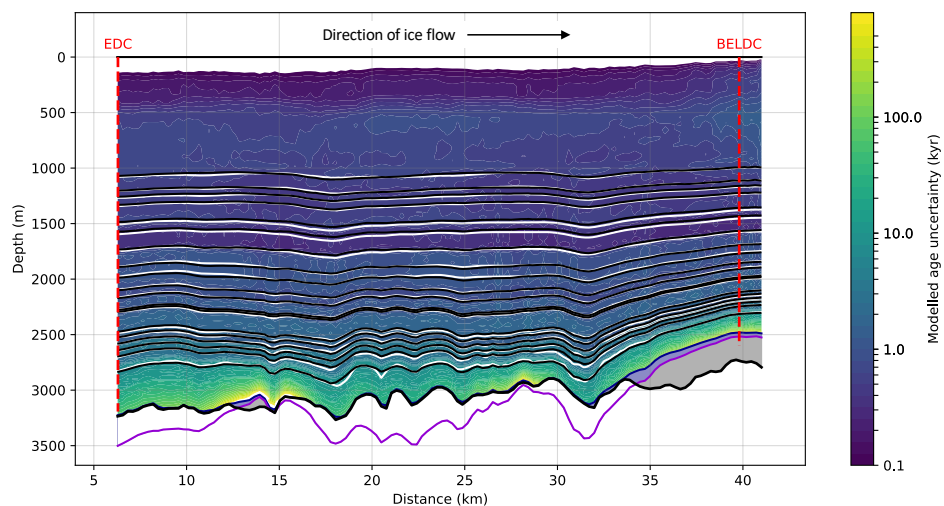


Figure S2. Age uncertainty from the 2.5D model for the DC–LDC flow line. White lines show observed isochrones mapped from the radar transect onto the flow line and black lines show modelled isochrones. The thick black line shows bedrock depth observed in the radar transect, the thick purple line is mechanical ice thickness H_m . Grey areas are modelled stagnant ice. The locations of the EDC and BELDC ice core drill sites are marked by red dashed lines. The present day direction of horizontal ice flow is left to right, from DC to LDC.

Age misfit

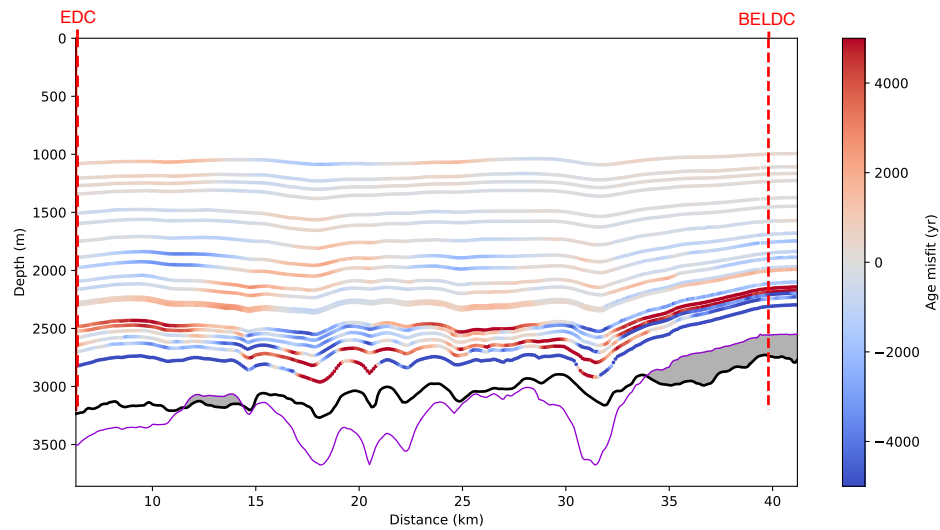


Figure S3. Age misfit for the 1D model from Chung et al. (2023a) applied to the DC–LDC flow line in this study. Age misfit corresponds to the age of modelled isochrones minus the age of observed isochrones. The thick black line shows bedrock depth observed in the radar transect, the thick purple line is mechanical ice thickness H_m . Grey areas are modelled stagnant ice. The locations of the EDC and BELDC ice core drill sites are marked by red dashed lines.